Temperature Dependence of the Crystal Structure and EPR Spectrum of Bis(1,3,5-Trihydroxycyclohexane)copper(II) Tosylate. A Unified Interpretation Using a Model of Dynamic Vibronic Coupling

Joachim Bebendorf,[†] Hans-Beat Bürgi,*[,‡] Eduard Gamp,[§] Michael A. Hitchman,*[,⊥] Angela Murphy,[‡] Dirk Reinen,*[,†] Mark J. Riley,[∥] and Horst Stratemeier[⊥]

Fachbereich Chemie und Zentrum für Materialwissenschaften der Philipps-Universität, D-35032 Marburg, Germany, Laboratorium für chemische und mineralogische Kristallographie, Universität Bern, Freiestrasse 3, CH-3012 Bern, Switzerland, Chemistry Department, Technikum Winterthur Ingenieurschule, CH-8400 Winterthur, Switzerland, Chemistry Department, University of Tasmania, Box 252C, Hobart, Tasmania 7001, Australia, and Chemistry Department, University of Queensland, Brisbane, Queensland 4072, Australia

Received March 29, 1996[⊗]

The crystal structure of bis(1,3,5-trihydroxycyclohexane)copper(II) tosylate is reported at temperatures of 293, 233, 188, 163, and 93 K, as are the structures of the Zn(II) and Ni(II) analogues at room temperature for comparison. The isomorphous compounds are triclinic, space group $P\bar{1}$, with one formula unit in the unit cell. The unit cell parameters of the Cu compound at 293 K are $a = 6.456(5)$ Å, $b = 9.505(3)$ Å, $c = 12.544(3)$ Å, $\alpha = 76.57(2)°$, $\beta = 87.48(4)°$, $\gamma = 76.65(4)°$. The centrosymmetric ZnO_6 and NiO_6 octahedra are tetragonally compressed with a slight orthorhombic distortion. The Cu^{2+} polyhedra exhibit similar geometries, but with considerably larger deviations from a regular octahedron. Two of the three independent Cu−O bond lengths and two of the *g*-values change significantly as a function of temperature. A model of dynamic vibronic coupling is presented which explains both the EPR and structural data. Vibronic wave functions associated with a Jahn−Teller potential energy surface modified by an orthorhombic lattice "strain" are given. The temperature dependence of the structures is calculated from the nuclear parts and that of the *g*-values from the electronic parts of the wave functions. The temperature dependence of the structures and *g*-values is also interpreted using a simpler model involving an equilibrium between two forms of the complex which differ solely in their orientation in the crystal lattice, and the results of the two approaches are compared.

1. Introduction

Six-coordinate complexes of Cu^{2+} invariably exhibit distortions away from the regular octahedral geometry adopted by most transition metal ions, this usually being ascribed to Jahn−Teller vibronic coupling. For six identical ligands, the distortion almost always produces a tetragonally elongated octahedron, with the highest energy electron occupying the $d_{x^2-y^2}$ orbital. However, orthorhombic and tetragonally compressed octahedral geometries are equally consistent with the Jahn−Teller theorem and are not much higher in energy. Because all of these geometries are connected via the motion of the ligands along the Jahn−Teller active vibrational coordinate, they may interconvert with relatively little input of energy. This makes Cu^{2+} complexes quite plastic,[1] and under certain circumstances the geometry and concomitant electronic structure changes as a function of temperature.[2] Observation of such behavior is important not only because it may indicate low-energy pathways involved in chemical reactions,[1] but also because Cu^{2+} proteins sometimes exhibit "dynamic" behavior;[3] moreover, it is possible that vibronic coupling of this kind plays a role in the mechanism underlying the behavior of the so-called "warm" superconductors.[4]

Fluxional Jahn−Teller distortions of Cu^{2+} complexes in the solid state imply a concerted change in both the vibrational and electronic wave functions, and these two features are generally investigated by quite different experimental techniques. In the first detailed investigation of a dynamic Cu^{2+} complex Bleaney and Bowers[5] studied the electronic structure of the $Cu(H_2O)_6^{2+}$ complex in Cu^{2+} doped $[Zn(H_2O)_6]SiF_6$ by electron paramagnetic resonance (EPR) spectroscopy. At room temperature, an isotropic EPR spectrum is observed, but on cooling to below ∼50 K a change to an anisotropic spectrum characteristic of the ground state of a tetragonally elongated octahedral complex occurs. In this, the axes of elongation are randomly distributed along the three mutually perpendicular Cu−H_2O bond directions. This illustrates the importance of the EPR time scale on the observations—at high temperatures, each complex fluctuates rapidly among the three orientations, but below ∼50 K the rate of exchange becomes smaller than the *g*-value anisotropy expressed in frequency units, so that the spectra associated with

* To whom correspondence should be addressed.
[†] Philipps Universität.
[‡] Universität Bern.
[§] Technikum Winterthur Ingenieurschule.
[⊥] University of Tasmania.
[∥] University of Queensland.
[⊗] Abstract published in *Advance ACS Abstracts,* October 15, 1996.

(1) Gazo, J.; Bersuker, I. B.; Garaj, J.; Kabesova, M.; Kahout, J.; Langfelderova, H.; Melnik, M.; Serator, M.; Valach, F. *Coord. Chem. Rev.* **1976**, *19*, 253. Hathaway, B. J. *Struct. Bonding (Berlin*) **1984**, *57*, 56.
(2) For recent discussions of the influence of Jahn−Teller coupling on Cu^{2+} stereochemistry, see: Reinen, D.; Atanasov, M. *Magn. Reson. Rev.* **1991**, *15*, 167. Hitchman, M. A. *Comments Inorg. Chem.* **1994**, *15*, 197.
(3) Bacci, M. *Struct. Bonding (Berlin)* **1983**, *55*, 67, and references cited therein.
(4) Fil, D. V.; Tokar, O. I.; Shelankov, A. L.; Weber, W. *Phys. Rev. B* **1992**, *45*, 5633. Englman, R.; Halperin, B.; Weger, M. *Solid State Commun.* **1989**, *70*, 57.
(5) Bleaney, B.; Bowers, K. D. *Proc. Phys. Soc. London (Ser. A)* **1952**, *65*, 667.

S0020-1669(96)00343-6 CCC: $12.00 © 1996 American Chemical Society

the different orientations can be resolved. In the $[Zn(H_2O)_6]SiF_6$ lattice, the metal is at a site of trigonal symmetry, so that the three orientations are crystallographically equivalent. In an important investigation, Silver and Getz extended the study by measuring the EPR spectrum of the $Cu(H_2O)_6^{2+}$ ion in the monoclinic unit cell of the Tutton salt $K_2[Zn(H_2O)_6](SO_4)_2$.[6] For each molecule, a spectrum characteristic of a tetragonally elongated complex with a small orthorhombic distortion was observed at low temperature, but on warming the signals associated with the two higher *g*-values gradually coalesced. This was explained in terms of a simple model (hereafter referred to as the SG model) in which all $Cu(H_2O)_6^{2+}$ ions possess identical geometries, but with the low symmetry of the lattice site rendering one of the three possible orientations higher in energy than the other two. These two orientations differ only slightly in energy, and, at 4 K, the EPR spectrum is characteristic of the orientation with the lowest energy. However, as the temperature is raised, a state becomes thermally populated in which the long Cu−O bond assumes an intermediate length and the intermediate bond becomes long. For each molecule, the frequency of exchange between these states is more rapid than the energy difference between the respective EPR signals, so that the observed spectrum is a population weighted average of two spectra. The third orientation is too high in energy to be populated at accessible temperatures. As just two bonds switch, only two molecular *g*-values are affected by temperature, the short Cu−O bond and lowest *g*-value being the same for the two orientations. The SG model was later used to interpret the temperature dependence of the EPR spectra of Cu^{2+} complexes present as dopants in a range of diamagnetic host lattices.[7]

To explore the behavior of these dynamic complexes in greater depth, Riley *et al.* developed a model (hereafter called the RHW model) to calculate the energy states and vibronic wave functions of a six-coordinate Cu^{2+} complex under the influence of both Jahn−Teller coupling and lattice strain interactions.[8,9] Initially, it was used to investigate the effect of the admixture of an upper state having the unpaired electron in the $d_{x^2-y^2}$ orbital upon the EPR spectrum of a complex essentially localized in a state with the unusual tetragonally compressed octahedral geometry and a d_{z^2} ground state.[8] Subsequently, to test the assumptions inherent in the simple SG approach, the model was applied to the EPR spectra of Tutton salts with a range of cations.[9] For the potassium salt, which was the subject of the original study, the vibronic wave functions calculated using the RHW model support the basic assumptions of the SG approach, that the temperature dependence of the EPR spectrum is dominated by the thermal population of two states corresponding essentially to different orientations of almost identical **g**-tensors. However, for Cu^{2+} doped into the Zn^{2+} Tutton salts of other countercations, the SG model appears to offer a somewhat poorer approximation. The factors influencing the vibronic wave functions were established, and the RHW model was used to quantify the strain induced upon the guest Cu^{2+} complex by the host lattice.

Information about the vibrational component of the vibronic wave functions of Jahn−Teller distorted Cu^{2+} complexes may be obtained from X-ray diffraction. With this technique two types of structural observables are accessible: (1) distances between the average positions of atoms and (2) atomic mean square displacements from mean positions.

Jahn−Teller distortions may affect both of these.[10−13] Though the expected tetragonally elongated octahedral geometry generally occurs, occasionally compounds having six identical copper−ligand bond lengths have been observed. This has sometimes led to the suggestion that the Jahn−Teller coupling is "quenched", though subsequent investigations have invariably found that the apparent cubic symmetry is the result of disorder between three polyhedra elongated along either the first, second, or third of the copper−ligand directions.[14] Similarly, crystal structure analyses sometimes indicate four long and two short copper−ligand bond lengths, and this has often been interpreted as indicating the presence of a complex with the unusual tetragonally compressed octahedral geometry with the unpaired electron in the d_{z^2} orbital.[15] Here, later work has usually shown that the *apparent* compressed tetragonal coordination geometry is due to a two-dimensional disorder between a pair of long and a pair of short copper−ligand bonds.[16] In all of these cases, the atomic displacement parameters of the disordered ligand atoms along the metal−ligand bond direction are significantly larger than those of the copper atom in the direction of the ligand atoms.[5] This is in contrast to the ordered structures, for which the two are much more similar. Measurement of the extended X-ray absorption fine structure (EXAFS) has proved valuable in this respect, as this gives the metal−ligand distances around each copper ion, rather than atomic positions averaged over the whole lattice.[17]

For certain compounds, the bond lengths indicated by the X-ray structure analysis are temperature dependent, behaving in a manner similar to the *g*-values of the $Cu(H_2O)_6^{2+}$ ion present as a dopant in the zinc Tutton salts. The mean square displacement parameters also show a temperature dependence, which is directly linked to the temperature dependence of the bond lengths.[12] The most extensive results are those reported by Simmons[14] for a range of compounds containing complexes of the general formula $[Cu(diamine)_2(O_2X)]^+$, where diamine is a chelating amine and O_2X a chelating oxyanion such as nitrite. The EPR behavior of such compounds, which has been summarized by Hathaway,[13] may be interpreted quite satisfactorily using the SG model. However, significant deviations are apparent for some compounds,[14] and it was speculated that these may be due to delocalization of the vibronic wave functions in an upper state involved in the thermal equilibrium. The Tutton salt $(NH_4)_2[Cu(H_2O)_6](SO_4)_2$ also shows dynamic behavior, this causing both the coordination polyhedron geometry and EPR spectrum to be temperature dependent.[18] Similar dynamic behavior is found for the deuterated form of this compound.[19] Of particular interest is the fact that the direction of the long and intermediate Cu−O bonds interchange upon deuteration; moreover for the deuterated compound switching of directions also occurs when the pressure is raised to 1.5 kbar.[20] While

(6) Silver, B. L.; Getz, D. *J. Chem. Phys.* **1974**, *61*, 638.
(7) Petrashen, V. E.; Yablokov, Yu. V.; Davidovitch, R. L. *Phys. Status Solidi B* **1980**, *101*, 117.
(8) Riley, M. J.; Hitchman, M. A.; Reinen, D. *Chem. Phys.* **1986**, *102*, 11.
(9) Riley, M. J.; Hitchman, M. A.; wan Mohammed, A. *J. Chem. Phys.* **1987**, *87*, 3766.
(10) Dunitz, J. D.; Orgel, L. E. *J. Phys. Chem. Solids* **1957**, *3*, 20. Cullen, D. L.; Lingafelter, E. C. *Inorg. Chem.* **1971**, *10*, 1264.
(11) Ammeter, J. H.; Bürgi, H. B.; Gamp, E.; Meyer-Sandrin, V.; Jensen, W. P. *Inorg. Chem.* **1979**, *18*, 733.
(12) Bürgi, H. B. *Trans. Am. Cryst. Assoc.* **1984**, *20*, 61. Stebler, M.; Bürgi, H. B. *J. Am. Chem. Soc.* **1987**, *109*, 1395.
(13) Hathaway, B. J. *Coord. Chem. Rev.* **1981**, *35*, 211.
(14) For a recent summary of crystallographic results on Jahn−Teller distortions in copper compounds, see: Simmons, C. J. *New J. Chem.* **1993**, *17*, 77.
(15) See, for example: Tucker, D.; White, P. S.; Trojan, K. L.; Kirk, M. L.; Hatfield, W. E. *Inorg. Chem.* **1991**, *30*, 823.
(16) Stratemeier, H.; Wagner, B.; Krausz, E. R.; Linder, R.; Schmidtke, H.-H.; Pebler, J.; Hatfield, W. E.; ter Haar, L.; Reinen, D.; Hitchman, M. A. *Inorg. Chem.* **1994**, *33*, 2320. Wagner, B.; Warda, S. A.; Hitchman, M. A. Reinen, D. *Inorg. Chem.*, in press.
(17) Ellis, P. J.; Freeman, H. C.; Hitchman, M. A.; Reinen, D.; Wagner, B. *Inorg. Chem.* **1994**, *33*, 1249.
(18) Alcock, N. W.; Duggan, M.; Murray, A.; Tyagi, S.; Hathaway, B. J.; Hewat, A. W. *J. Chem. Soc., Dalton Trans.* **1984**, 7.
(19) Hathaway, B. J.; Hewat, A. W. *J. Solid State Chem.* **1984**, *51*, 364.

this overall behavior may be explained reasonably well in general terms using the RHW model,[20] significant deviations are observed at higher temperatures, and it has been suggested that these are probably due to cooperative interactions.

Cooperative effects are expected in compounds where the coordination polyhedra are so close that a thermally (or pressure) induced structural change at one lattice site will influence the potential surface of its neighbors. The interactions are cushioned if the ligands and counterions are relatively large and "soft", features which were exploited in a study of the compound $[Cu(tach)_2]X_2$, where tach = *cis,cis*-1,3,5-triaminocyclohexane and $X = NO_3^-$ and ClO_4^-.[11] Here, the EPR spectra between 4 and 300 K, and the atomic displacement (or thermal ellipsoid) parameters of the ligand donor atoms derived from the X-ray structure analysis at room temperature, were analyzed in terms of tetragonally elongated octahedral complexes in which disorder of the long bonds over three orientations is governed by a temperature dependent dynamic equilibrium.

The temperature dependence of the EPR spectrum reported[23] for the similar compound $[Cu(thch)_2](tos)_2$, thch = *cis,cis*-1,3,5-trihydroxycyclohexane, tos = tosylate, suggested that significant cooperative effects are absent. This compound is therefore a good candidate for testing the extension of the RWH model to the simultaneous treatment of both EPR and structural data. We have determined the crystal structure of the compound at five temperatures between 93 and 293 K and analyzed the Cu−O bond distances, the Cu and O atomic displacement parameters, and the molecular *g*-values in terms of a dynamic equilibrium between the vibronic wave functions of a Jahn−Teller system perturbed by a lattice strain. The results are compared with those obtained using the simpler SG approach. The crystal structures of the analogous zinc and nickel compounds at room temperature were also determined to allow comparison with complexes formed by non-Jahn−Teller active metal ions.

2. Experimental Section

2.1. Preparation of Compounds. $[Cu(thch)_2](tos)_2$. Anhydrous $CuCO_3$ (2.22 g, 18 mmol) was dissolved in hydrated toluene-4-sulfonic acid monohydrate (6.84 g, 36 mmol) and the mixture stirred for 3 h until evolution of CO_2 ended. The solution was filtered and left to stand at room temperature for several hours, when light blue crystals of $Cu(tos)_2$ formed. These were filtered off, washed with a little cold ethanol, and dried. This compound (2.21 g, 5 mmol) was dissolved in ethanol (30 mL) and the solution added to one of *cis,cis*-1,3,5-trihydroxycyclohexane dihydrate (1 g, 7.56 mmol, Aldrich) in ethanol (20 mL). The resulting solution was kept at 70 °C for several hours, when blue crystals of the desired product $[Cu(thch)_2](tos)_2$ formed. These were recrystallized from aqueous ethanol. Anal. Found (calcd for $C_{26}H_{38}O_{12}S_2Cu$ in parentheses): C, 46.9 (46.59); H, 5.6 (5.71); Cu, 9.3 (9.48).

$[Ni(thch)_2](tos)_2$. Basic nickel carbonate, $Ni_2(OH)_2CO_3 \cdot 4H_2O$ (2.67 g, 10 mmol) was dissolved in hydrated toluene-4-sulfonic acid monohydrate (7.61 g, 40 mmol) and the mixture stirred for about 5 h until evolution of CO_2 ended. The solution was filtered and left to stand at room temperature for 24 h, when green crystals of $Ni(tos)_2$ formed. These were filtered off, washed with a little cold ethanol, and dried. This compound (2.40 g, 5 mmol) was dissolved in ethanol (30 mL) and the solution added to one of *cis,cis*-1,3,5-trihydroxycyclohexane dihydrate (1.68 g, 10 mmol; Aldrich) in ethanol (30 mL). The resulting solution was kept at 70 °C for several hours, when light green crystals of the desired product $[Ni(thch)_2](tos)_2$ formed. These were recrystallized from aqueous ethanol. Anal. Found (calcd for $C_{26}H_{38}O_{12}S_2Ni$ in parentheses): C, 46.9 (46.89); H, 5.9 (5.72); Ni, 8.5 (8.82).

$[Zn(thch)_2](tos)_2$. Zinc powder (1.82 g, 28 mmol) was dissolved in hydrated toluene-4-sulfonic acid monohydrate (10.61 g, 56 mmol) and the mixture stirred for about 24 h until evolution of H_2 ended. The solution was filtered and left to stand at room temperature for several hours, when colorless crystals of $Zn(tos)_2$ formed. These were filtered off, washed with a little cold ethanol, and dried. This compound (2.22 g, 5 mmol) was dissolved in ethanol (30 mL) and the solution added to one of *cis,cis*-1,3,5-trihydroxycyclohexane dihydrate (1 g, 7.56 mmol; Aldrich) in ethanol (20 mL). The resulting solution was kept at 70 °C for several hours, when the product $[Zn(thch)_2](tos)_2$ formed as a white microcrystalline powder. Larger crystals were obtained by slowly cooling a solution in ethanol. Anal. Found (calcd for $C_{26}H_{38}O_{12}S_2Zn$ in parentheses): C, 46.5 (46.42); H, 5.8 (5.65); Zn, 9.4 (9.74).

2.2. Optical Measurements. Electronic reflectance spectra were recorded using a Zeiss PMQ II spectrophotometer with a low-temperature attachment, using freshly sintered MgO as a standard. The extent of reflection was transformed into absorption intensity data $\log(k/s)$ (k and s are absorption and scattering coefficients, respectively) using the theory of Kubelka−Munk.[24]

2.3. X-ray Diffraction Measurements. Three single crystals of $[Cu(thch)_2](tos)_2$ were studied by X-ray diffraction, one at 93 K, one at 293 K, and one at 163, 188, and 233 K. Crystals of the corresponding Zn^{2+} and Ni^{2+} compounds were studied at 293 K. The data were subjected to Lorentz and polarization corrections. All atoms except hydrogen were refined anisotropically. The weighted reliability factors are <0.04 except for the Zn^{2+} compound. Several crystals of this were studied, but the quality of the structure determination could not be improved. Since the geometry of the ZnO_6 polyhedron is probably reliable, the origin of the difficulties was not pursued further. Experimental details on all determinations are summarized in Table 1, with further details being given in Supporting Information Table S1. Complete listings of atomic coordinates, bond lengths, bond angles, and displacement parameters are given in Supporting Information Tables S2−S4.

3. Results and Discussion

3.1. Crystal Structures. The compounds $[M(thch)_2](tos)_2$, M = Cu, Zn, Ni, are isomorphous (Table 1) and have one formula unit in the triclinic unit cell (Figure 1). The metal lies on an inversion center so that the complexes formed by the two trihydroxy ligands are rigorously centrosymmetric. The geometry of the $[Cu(thch)_2]^{2+}$ complex at 233 K is shown in Figure 2. The angles O−M−O are in the range 84−90°, quite close to that expected for a regular octahedron. The metal−oxygen bond lengths (Table 2) follow the sequence M−O2 > M−O3 > M−O1, though the differences are much larger for Cu than for Zn and Ni (indeed, for the Ni and Zn complexes, the difference between the bonds to O2 and O3 is less than three times the experimental uncertainty). As the three hydroxy groups of the tridentate ligand are chemically equivalent, the bond length differences may be ascribed to interactions with the surrounding lattice, with these being dramatically amplified and modified by Jahn−Teller coupling in the case of the copper complex. This aspect is discussed more fully in sections 3.2 and 3.4 The geometry of the copper complex alters significantly between 293 and 93 K. The difference between the Cu−O2 and Cu−O3 bond lengths more than doubles on cooling, though their mean remains constant. The Cu−O1 bond length is essentially temperature invariant.

This behavior is similar to that reported by Simmons[14] for a range of complexes of the type $[Cu(diamine)_2(O_2X)]^+$, where the behavior was ascribed to a temperature dependent equilibrium between two "structural isomers" which have very similar geometries but different energies. Applying similar reasoning to the present compound, the low-energy conformer has a long bond to O2 and a much shorter bond to O3, while the reverse is true for the high-energy conformer. At any particular

(20) Simmons, C. J.; Hitchman, M. A.; Stratemeier, H.; Schultz, A. J. *J. Am. Chem. Soc.* **1993**, *115*, 11304.
(21) Sheldrick, G. M. *SHELXTL*, Program for Crystal Structure Determinations; University of Cambridge: Cambridge, U.K., 1992.
(22) (a) Cromer, D. T.; Mann, J. B. *Acta Crystallogr.* **1968**, *A24*, 321. (b) Cromer, D. T.; Libermann, D. *J. Chem. Phys.* **1970**, *53*, 1891.
(23) Gamp, E. Ph.D. Thesis (No. 6673), Eidgenössische Technische Hochschule, Zürich, 1980.
(24) See: Kortim, G. *Angew. Chem.* **1955**, *67*, 694.

Table 1. Crystallographic Data for $[Cu(thch)_2](tos)_2$, $[Ni(thch)_2](tos)_2$, and $[Zn(thch)_2](tos)_2$

	$[Cu(thch)_2](tos)_2$					$[Ni(thch)_2](tos)_2$	$[Zn(thch)_2](tos)_2$
formula			$C_{26}H_{38}O_{12}S_2Cu$			$C_{26}H_{38}O_{12}S_2Ni$	$C_{26}H_{38}O_{12}S_2Zm$
fw	670.254	670.254	670.254	670.254	670.254	665.424	672.084
space groups	$P\bar{1}$ (No. 2)	$P\bar{1}$ (No. 2)	$P\bar{1}$ (No. 2)	$P\bar{1}$ (No. 2)	$P\bar{1}$ (No. 2)	$P\bar{1}$ (No. 2)	$P\bar{1}$ (No. 2)
a, Å	6.385(4)	6.411(1)	6.422(1)	6.431(7)	6.456(5)	6.453(1)	6.458(2)
b, Å	9.401(7)	9.451(1)	9.464(1)	9.478(1)	9.505(3)	9.504(1)	9.549(1)
c, Å	12.410(9)	12.466(3)	12.475(1)	12.503(1)	12.544(3)	12.515(1)	12.526(3)
α, deg	76.82(6)	76.66(1)	76.66(1)	76.65(1)	76.57(2)	76.73(2)	76.48(1)
β, deg	87.68(5)	87.55(2)	87.52(1)	87.50(1)	87.48(4)	86.47(1)	86.62(1)
ψ, deg	77.06(6)	76.78(1)	76.77(1)	76.73(1)	76.65(4)	76.92(1)	77.08(2)
V, Å^3	706.83	715.42	718.13	721.67	728.43	727.62	732.01
Z	1	1	1	1	1	1	1
temp, K	93	163	188	233	293	293	293
λ, Å	0.710 73	1.5418	1.5418	1.5418	0.710 73	1.5418	1.5418
D_c, g cm^{-3}	1.574	1.56	1.55	1.54	1.521	1.50	1.51
μ, cm^{-1}	9.8	29.9	29.8	29.7	9.8	27.9	30.1
R^a	0.026	0.034	0.035	0.041	0.034	0.052	0.110
$R_w{}^a$	0.033	0.033	0.036	0.039	0.044	0.040	0.086

[a] Definitions of R and R_w: $R = \sum||F_o| - |F_c|/\sum|F_o|$; $R_w = \{\sum w(|F_o| - |F_c|)^2/\sum wF_o^2\}^{1/2}$.

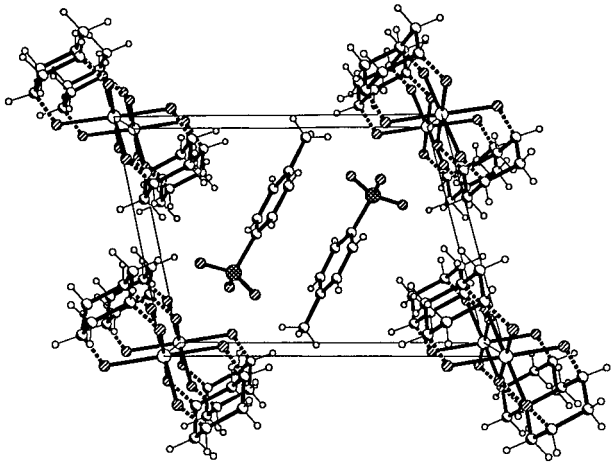

Figure 1. View of the unit cell of $[Cu(thch)_2](tos)_2$ down the *a* axis at 233 K.

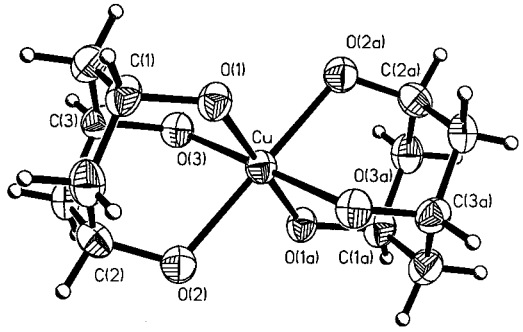

Figure 2. Molecular structure of $[Cu(thch)_2]^{2+}$ at 233 K showing labeling of the atoms and with 50% thermal displacements indicated.

temperature, the observed bond distances are the average of these, weighted by their thermal populations. This aspect is considered quantitatively in sections 3.2 and 3.5.

The effect of a substantial population of the higher energy form on the atomic displacement parameters is more subtle but can be clearly discerned from the experimental data. The population of two (tetragonally elongated) conformers not only causes a change in the average oxygen positions but also a concomitant "smearing" of four of the ligand atoms along the respective copper ligand vectors and thus an extra contribution to the total mean square ligand displacements. Qualitatively, the difference ΔU between the mean square displacements of the ligand atoms and the copper atom along the copper−ligand direction should increase with increasing disorder, *i.e.*, with increasing temperature. This is indeed observed (Table 3). Note

Table 2. Metal−Oxygen Bond Lengths in the Complexes (Å, Standard Deviation in Parentheses)[a]

		M−O1		M−O2		M−O3	
metal	temp	obsd	calcd	obsd	calcd	obsd	calcd
Cu	293	1.974(2)	1.973	2.167(2)	2.178	2.079(2)	2.072
Cu	233	1.974(3)	1.971	2.192(3)	2.188	2.064(3)	2.064
Cu	188	1.969(3)	1.971	2.196(3)	2.196	2.056(3)	2.056
Cu	163	1.972(2)	1.971	2.211(2)	2.204	2.052(2)	2.048
Cu	93	1.968(2)	1.971	2.223(2)	2.222	2.021(2)	2.029
Ni	293	2.047(4)		2.063(4)		2.060(4)	
Zn	293	2.049(11)		2.084(8)		2.073(9)	

[a] See Figure 6, surface b, for the parameters used to obtain the calculated values.

Table 3. Observed and Calculated Mean Square Displacement Parameters

(a) Differences between Observed Mean Square Displacements of Ligand and Metal Atoms along the Ligand−Metal Vectors

T, K	Cu−O1, Å^2	Cu−O2, Å^2	Cu−O3, Å^2	*σ*, Å^2
93	0.0021	0.0021	0.0041	0.0007
163	0.0010	0.0041	0.0025	0.0010
188	0.0028	0.0061	0.0041	0.0015
233	−0.0021	0.0055	0.0040	0.0020
293	0.0030	0.0117	0.0132	0.0007

(b) Calculated Mean Square Displacements $\langle d_x^2\rangle - \langle d_x\rangle^2$, etc.

T, K	Cu−O1, Å^2	Cu−O2, Å^2	Cu−O3, Å^2
90	0.0008	0.0020	0.0021
160	0.0010	0.0048	0.0050
190	0.0011	0.0058	0.0060
230	0.0013	0.0068	0.0070
290	0.0020	0.0080	0.0081
350	0.0023	0.0088	0.0088

that the increase in ΔU is small compared to the increase of the atomic displacement parameters in general, most of which is due to molecular librations and translations. The disorder effect is therefore easily overlooked unless the displacement parameters are analyzed in terms of the differences ΔU along the copper ligand vectors.[11] The ΔU's are small for all Cu−O bonds at 93 K where there is little or no disorder, and they are smallest for the Cu−O1 bond at all temperatures since this distance is temperature independent. Average ΔU's for the Ni and Zn compounds, which show no Jahn−Teller distortions, are also small, −0.0040(30) and 0.0015(70) Å^2, but much less reliable.

The complexes stack one above another approximately along the *a* axis, as may be seen from Figure 1. The tosylate anions are interspaced between the complexes in the *b*,*c*-plane, so that the metal centers are well-separated. The Cu−O2 and Cu−O3

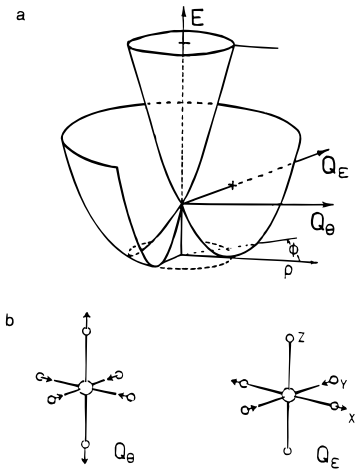

Figure 3. (a) "Mexican hat" potential surface formed by $e_g \times E_g$ Jahn−Teller coupling. (b) Form of the Jahn−Teller active ϵ_g vibrations.

bonds involved in the dynamic equilibrium lie approximately in this plane, so that when the bond lengths in any particular complex change, this will have relatively little effect on neighboring complexes. Thus, cooperative interactions are expected to be small, and the thermal behavior can be interpreted in terms of a Boltzmann distribution of isolated complexes.

3.2. Vibronic Coupling Model and Temperature Dependence of the Structural Parameters. The temperature dependence of the bond lengths of the $[Cu(thch)_2]^{2+}$ complex shows a similar trend to that observed for the *g*-values of Cu^{2+} doped into a range of Tutton salts. The RHW vibronic coupling model successfully used for the Tutton salts,[9] and described in detail elsewhere,[8,9] was therefore extended to allow the treatment of bond lengths.

The deviation from a regular octahedral geometry of a complex distorted by $E_g \times \epsilon_g$ Jahn−Teller coupling is most easily described in terms of displacements Q_θ and Q_ϵ corresponding to the ϵ_g normal coordinates (Figure 3b). The displacements, and the corresponding composition of the electronic part of the ground state wavefunction, ψ_e, can also be expressed in terms of polar coordinates (Figure 3a).

$$Q_\theta = \rho \cos\phi, \quad Q_\epsilon = \rho \sin\phi \tag{1a}$$

$$\psi_e = d_{x^2-y^2} \cos(\phi/2) + d_{z^2} \sin(\phi/2) \tag{1b}$$

The general form of the potential energy surface takes into account the coupling between the ^2E_g electronic state and the Jahn−Teller active ϵ_g vibrational mode of the parent octahedral complex (parameters A_1, A_2, ν) as well as the strain imposed on it by the surrounding lattice (S_θ, S_ϵ).

$$V = h\nu\rho^2/2 + \rho[A_1^{\,2} + 2A_1A_2\rho\cos(3\phi) + A_2^{\,2}\rho^2 + (S_\theta^{\,2} + S_\epsilon^{\,2})/\rho^2 + 2S_\theta(A_1/\rho\cos\phi + A_2\cos(2\phi)) + 2S_\epsilon(A_1/\rho\sin\phi - A_2\sin(2\phi))]^{1/2} \tag{2}$$

The various parameters are conventionally measured in cm^{-1} except for the radial distortion parameter ρ which is dimensionless. To first order, a complex with six identical ligands undergoes a radial distortion in the ϵ_g modes. The distortion is driven by the linear coupling A_1 and leads to the "Mexican hat" potential surface pictured in Figure 3a. At this level of approximation, the coupling to the Q_θ and Q_ϵ components of the ϵ_g vibration, pictured in Figure 3b, is energetically equivalent, and the energy minimum is a circular well of radius ρ_0. Higher order effects, represented in the model by the parameter A_2, cause a "warping" of the Mexican hat potential surface to give three equivalent minima at $\phi = 0°$, 120°, and 240°, each of which corresponds to a tetragonally elongated geometry with a $d_{x^2-y^2}$ type ground state (see Figure 6 and section 3.4). The extent of the warping is normally expressed by the parameter β, a function of A_2, where the energy difference between the minima and saddlepoints in the well is given by 2β. In a low-symmetry environment such as a triclinic crystal, the geometry of the complex is not solely determined by the Jahn−Teller effect but also by lattice packing forces, so that the three minima are no longer equal in energy. This may be parametrized in terms of the lattice strain components S_θ and S_ϵ.

The vibronic wave functions which result from the diagonalization of the vibronic matrix[8,9] are products of an electronic part and two one-dimensional harmonic oscillator basis functions $|i\rangle|j\rangle$ (eq 3). Here, i, j can take the values 0, 1, ..., n_e, where n_e is the cutoff for the vibrational basis functions. In the present calculations $n_e = 57$, which gives a total vibronic basis of 3422.

$$\Psi = \sum_{ij} a_{ij}|d_{x^2-y^2}\rangle|i\rangle|j\rangle + b_{ij}|d_{z^2}\rangle|i\rangle|j\rangle \tag{3}$$

The appropriate expectation values are obtained by integration over the nuclear coordinates. It is convenient to calculate expectation values of powers of the (dimensionless) normal coordinates, where the quantities $\langle Q\rangle$ and $\langle Q^2\rangle$ can be related to the atomic positions and the internal mode contributions to the thermal ellipsoids, respectively, as obtained from the crystal structure analysis.[25] The expectation value of Q^n in the state Ψ is given by

$$\langle Q^n\rangle = \langle\Psi|Q^n|\Psi\rangle = \sum_{iji'j'} a_{ij}a_{i'j'}\langle j|\langle i|Q^n|i'\rangle|j'\rangle + b_{ij}b_{i'j'}\langle j|\langle i|Q^n|i'\rangle|j'\rangle \tag{4}$$

Simple expressions are available[26] for the matrix elements of the one-dimensional harmonic oscillator basis with powers of the coordinate.

$$\langle i|j\rangle = \delta_{i,j}$$

$$\langle i|Q|j\rangle = \left(\frac{i}{2}\right)^{1/2}\delta_{i-1,j} + \left(\frac{i+1}{2}\right)^{1/2}\delta_{i+1,j}$$

$$\langle i|Q^2|j\rangle = \frac{1}{2}(i(i-1))^{1/2}\delta_{i-2,j} + \left(i+\frac{1}{2}\right)\delta_{i,j} + \frac{1}{2}((i+1)(i+2))^{1/2}\delta_{i+2,j} \tag{5}$$

The calculation of these expectation values can also be achieved by direct numerical integration using (for example) Gaussian quadrature formulas. This takes far more computer time but allows an independent check of the results.

For cubic systems, where the strain terms are zero, the expectation values $\langle Q_\theta\rangle = \langle Q_\epsilon\rangle = 0$. That is, the average geometry in a dynamic Jahn−Teller system is that of the high-symmetry cubic geometry. However, the mean-squared expectation values $\langle Q_\theta^2\rangle$, $\langle Q_\theta Q_\epsilon\rangle$ and $\langle Q_\epsilon^2\rangle$ are nonzero. These have been used, for example, to interpret the thermal ellipsoids of the Jahn−Teller $Cu(NO_2)_6^{4-}$ system[10,11] and to explain the mean-squared amplitudes of VCl_4 in the gas phase.[27] There is an approximate relationship between mean-squared values and the position of the minima of the potential energy surface $\langle Q_\theta^2\rangle$

(25) Willis, B. T. M.; Pryor, A. W. *Thermal Vibrations in Crystallography*; Cambridge University Press: Cambridge, U.K., 1975.
(26) Shaffer, W. H.; Krohn, B. J. *J. Mol. Spectrosc.* **1976**, *63*, 323.
(27) Morino, Y.; Uehara, H. *J. Chem. Phys.* **1966**, *45*, 4543.

$+ \langle Q_\epsilon^2 \rangle = \langle \rho^2 \rangle \approx \rho_0^2$ for linear Jahn−Teller coupling.[11] This approximation is best when first-order coupling is large.

The relationships of the Q_θ, Q_ϵ coordinates to the mass- and energy-weighted ligand displacements *x*, *y*, *z* are given by

$$\begin{pmatrix} \langle x \rangle \\ \langle y \rangle \\ \langle z \rangle \end{pmatrix} = \begin{pmatrix} -\sqrt{1/12} & 1/2 \\ -\sqrt{1/12} & -1/2 \\ \sqrt{1/3} & 0 \end{pmatrix} \begin{pmatrix} \langle Q_\theta \rangle \\ \langle Q_\epsilon \rangle \end{pmatrix} \tag{6}$$

$$\begin{pmatrix} \langle x^2 \rangle & \langle xy \rangle & \langle xz \rangle \\ \langle xy \rangle & \langle y^2 \rangle & \langle yz \rangle \\ \langle xz \rangle & \langle yz \rangle & \langle z^2 \rangle \end{pmatrix} = \begin{pmatrix} -\sqrt{1/12} & 1/2 \\ -\sqrt{1/12} & -1/2 \\ \sqrt{1/3} & 0 \end{pmatrix} \times \begin{pmatrix} \langle Q_\theta^2 \rangle & \langle Q_\theta Q_\epsilon \rangle \\ \langle Q_\theta Q_\epsilon \rangle & \langle Q_\epsilon^2 \rangle \end{pmatrix} \begin{pmatrix} -\sqrt{1/12} & -\sqrt{1/12} & \sqrt{1/3} \\ 1/2 & -1/2 & 0 \end{pmatrix} \tag{7}$$

Here the displacements $\langle x \rangle$, $\langle y \rangle$, and $\langle z \rangle$ are relative to the ideal octahedral geometry without Jahn−Teller distortion. The mean square displacements $\langle x^2 \rangle$, $\langle y^2 \rangle$, and $\langle z^2 \rangle$ are related to the ΔU's obtained from single crystal diffraction experiments as explained in section 3.1 and eq 8 below. The covariance terms $\langle xy \rangle$, $\langle xz \rangle$, and $\langle yz \rangle$, however, cannot be observed in such an experiment. The mass- and energy-weighted displacements *x etc.* may be transformed into absolute displacements d_x *etc.* by

$$d_x\,(\text{Å}) = \frac{5.80648}{(Mh\nu)^{1/2}}\, x \tag{8}$$

Here d_x is the coordinate, *M* is the mass of one ligand in amu, and $h\nu$ is the energy of the ϵ_g vibration in cm^{-1}.

To a first approximation, the magnitude of the distortion of a complex from a regular octahedral geometry is determined by the Jahn−Teller interaction, while the preferred direction of distortion is decided by the strain. Even small strain terms will be vibronically enhanced and have a large effect on the geometry. To obtain the molecular geometry at any temperature, the expectation values of the coordinates are calculated using eq 4. From this, the changes in ligand geometry for a particular vibronic state are estimated using eqs 6 and 8. This is repeated for all levels that are thermally populated and a Boltzmann average taken. The temperature dependent mean geometry is then compared with experiment. Similarly, the temperature dependent mean-squared geometry may be obtained using eqs 7 and 8. Note, however, that in the case of strain $\langle x \rangle$, $\langle y \rangle$, and $\langle z \rangle$ are not necessarily zero; therefore the mean square deviations are $\langle (x - \langle x \rangle)^2 \rangle = \langle x^2 \rangle - \langle x \rangle^2$, *etc.*, rather than just $\langle x^2 \rangle$, *etc*.

To apply this model to $[Cu(thch)_2]^{2+}$, the parameters describing the Jahn−Teller coupling ($h\nu$, *M*, A_1, A_2) and the influence of the strain (S_θ, S_ϵ) must be estimated. The approach is basically similar to that discussed previously[9] for the copper(II) Tutton salts. The symmetry of an isolated, undistorted $[Cu(thch)_2]^{2+}$ complex is expected to be D_3, so that the three wells of the warped Mexican hat potential surface remain symmetry equivalent as implied in our model. The structures of the Zn and Ni complexes are indeed close to this geometry. The architecture of the bulky, tridentate ligand may influence the linear coupling A_1, the vibrational constants $h\nu$, *M*, and possibly the warping parameter β (A_2), but will not contribute directly to the strain interactions, which solely reflect the influence of the surrounding lattice upon the complex.

The overall distortion of the $[Cu(thch)_2]^{2+}$ complex is considerably smaller than that observed for $Cu(H_2O)_6^{2+}$, presumably because of the rigidity of the tridentate trihydroxycyclohexane ligand. After a small correction is made for the thermal population of upper vibronic states (see below), the degree of distortion R_{JT} can be estimated from the absolute displacements of the bond lengths d_x, *etc.*, from their average:

$$R_{JT} = (2d_{x^2} + 2d_{y^2} + 2d_{z^2})^{1/2}$$

The distortion is $R_{JT} = 0.271$ Å for $[Cu(thch)_2]^{2+}$, which is ∼30% lower than the distortion of 0.39 Å observed for the $Cu(H_2O)_6^{2+}$ ion.[28] The transformation from R_{JT} to ρ_0 follows from (eq 8); it is

$$\rho_0 = R_{JT}(Mh\nu)^{1/2}/5.806$$

The overall Jahn−Teller distortion ρ_0 depends upon the linear coupling constant A_1 and inversely upon the energy $h\nu$ of the ϵ_g vibration. Hence, the smaller distortion of the $[Cu(thch)_2]^{2+}$ ion compared with that of $Cu(H_2O)_6^{2+}$ might be due to either or both of these factors. It is assumed that they contribute approximately equally to the reduction. The linear coupling constant was reduced by ∼15% compared with the value $A_1 = 900\ cm^{-1}$ deduced for $Cu(H_2O)_6^{2+}$,[9] leading to the value ∼750 cm^{-1} for $[Cu(thch)_2]^{2+}$. Unfortunately, the energy of the ϵ_g mode cannot be obtained directly from the Raman spectrum of $[Zn(thch)_2](tos)_2$, as the intensity of the peak is expected to be very low, and the ligand and tosylate anion both exhibit rich spectra in the region of interest. It was therefore estimated in the following manner. The energy of the ϵ_g mode depends both upon its force constant *f* and the ligand mass *M* via the relationship

$$h\nu \propto (f/M)^{1/2}$$

The force constant of the ϵ_g vibration of $[Cu(thch)_2]^{2+}$ was taken to be 20% higher than that of $Cu(H_2O)_6^{2+}$. For a polyatomic ligand like thch, the ligand mass involved in the distortion is uncertain. It is presumably somewhat higher than the value of 17 amu for a hydroxy group, and a mass of 25 was used in the calculations. Here, the ligand mass basically acts as a scaling factor. The combination of an effective ligand mass of 25 and a 20% increase in force constant leads to an energy $h\nu \approx 280\ cm^{-1}$ for the $[Cu(thch)_2]^{2+}$ complex, compared with the value of 300 cm^{-1} for the hexahydrate ion.[9] It should be noted that the representation of the polyatomic ligand by single atoms represents a rather serious approximation, so that the vibrational energy and ligand mass must both be considered to be "effective parameters".

A check on the self-consistency of the parameters is provided by the energies of the excited electronic states of $[Cu(thch)_2](tos)_2$ as obtained from its reflectance spectrum (Figure 4). At low temperature, this consists of a broad double band at ∼10 500 and 13 000 cm^{-1} and and a broad peak at ∼6000 cm^{-1} overlayed by a number of much sharper features. Comparison with the spectrum of $[Zn(thch)_2](tos)_2$ provides evidence that the sharp peaks below 9000 cm^{-1} are due to overtones of vibrational transitions. The following band assignments are therefore made: $^2B_{1g}(x^2-y^2) \rightarrow {}^2A_{1g}(z^2)$ at ∼6000 cm^{-1}, $^2B_{2g}(xy)$ at ∼10 500 cm^{-1}, and $^2E_g(xz,yz)$ at 13 000 cm^{-1} (the singly occupied d-orbitals are indicated in brackets, and for simplicity, symmetry labels appropriate to a complex of D_{4h} symmetry are used). The energy of the first band, which equals the splitting of the parent ^2E_g state, is distinctly lower than the value of ∼7500 cm^{-1} observed for the $Cu(H_2O)_6^{2+}$ complex.[29] The

(28) Deeth, R. J.; Hitchman, M. A. *Inorg. Chem.* **1986**, *25*, 1225.

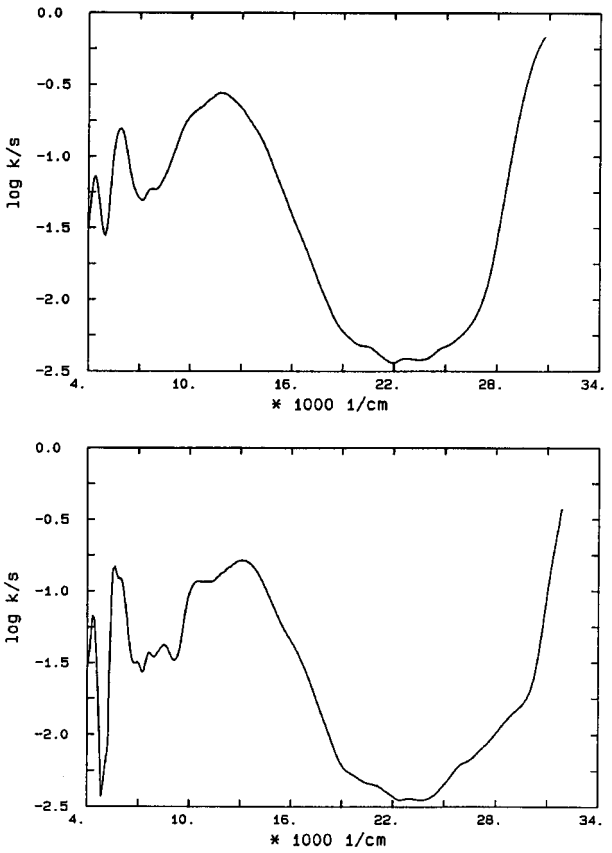

Figure 4. Electronic reflectance spectrum of $[Cu(thch)_2](tos)_2$ at 5 (top) and 295 K (bottom). The sharp features below ~9000 cm^{-1} are due to vibrational transitions of the ligand and tosylate anion.

ligand field splitting parameter $\Delta \approx 9000$ cm^{-1} estimated for the parent octahedral Cu^{2+} complex using the center-of-gravity rule compares well with that observed for the corresponding Ni^{2+} complex ($\Delta = 9500$ cm^{-1}, $B = 890$ cm^{-1}).

If higher-order interactions are neglected, the splitting, ΔE, of the parent octahedral ^2E_g state is given[2] by the relationship $\Delta E \approx 2A_1\rho_0$. The parameter values chosen here yield the estimate $\Delta E = 5840$ cm^{-1} in good agreement with the observed transition energy, ~6000 cm^{-1}.

The warping of the potential surface is represented in the calculation by a second order electronic coefficient A_2, which is related to the parameter β by the approximation[9]

$$\beta \cong A_2{A_1}^2/(h\nu)^2$$

Estimates of β vary widely, from close to 0 for Cu^{2+}-doped MgO,[30] to 50−100 cm^{-1} in doped zinc(II) fluoride[8,31] and NH_4-Cl lattices,[32] to 300−600 cm^{-1} for the $Cu(H_2O)_6^{2+}$ and $CuCl_6^{4-}$ ions.[9,16,33] The size of the warping is apparently a balance between several competing factors,[2,28] and it has been suggested[28] that β is likely to be larger for complexes involving isolated ligands than those in continuous lattices. A range of values was explored in the present calculations, and a value of $\beta \approx 230$ cm^{-1} was found to agree best with experiment.

While the above parameters define the basic warped Mexican hat potential surface of the $[Cu(thch)_2]^{2+}$ complex, the orthorhombicity of the bond lengths and the way in which they vary with temperature are predominantly decided by the strain produced by the surrounding lattice (see Figure 6 and the discussion in section 3.4). The axial component of the strain, S_θ, is clearly negative, corresponding to a compression acting along the direction of the short Cu−O1 bonds. The bond length anisotropy was found to be quite sensitive to the ratio of β to S_θ, as expected when these are opposite in sign.[34] As noted in previous studies involving EPR spectra,[9,34] this ratio largely defines the position of the lowest minimum in the "trough" of the Mexican hat potential surface, and for $[Cu(thch)_2](tos)_2$ the bond length anisotropy observed at low temperature implies the ratio $|S_\theta|/\beta \approx 2.2$. With $\beta \approx 230$ cm^{-1}, this yields the value $S_\theta \approx -500$ cm^{-1}.

The temperature dependence of the long and intermediate bond lengths depends upon the energy difference between the two lower minima in the potential surface, and this is decided largely by the orthorhombic component of the axial strain. A value of $S_\epsilon = 150$ cm^{-1} produces good agreement with experiment. A deviation of ~10% in S_ϵ produced a noticeable worsening of this agreement. The variation of the bond lengths calculated using the above optimum parameters is compared with the experimental values in Figure 5a (solid line).

Although the ratio $|S_\theta|/\beta$ may be fixed reasonably accurately as described above, the absolute values of these parameters are much harder to quantify. In setting limits for these, it may be noted that the axial strain is the dominant factor influencing the energy of the highest of the three minima in the ground state potential surface (see Figure 6 and section 3.4). If this is thermally populated, all three metal−ligand bond lengths are temperature dependent. Lower limits for S_θ and β follow from the fact that the shortest Cu−O distance of $[Cu(thch)_2](tos)_2$ does not vary significantly with temperature. Thus, if S_θ is changed to -220 cm^{-1} and β to 100 cm^{-1} (dotted−dashed lines on Figure 5a), the shortest bond increases in length at high temperature, in contrast to experiment. Since the overall Jahn−Teller radius ρ_0 is somewhat sensitive to β, and in order to maintain ρ_0 at the experimental value, the linear coupling constant and energy of the ϵ_g mode must be changed to $A_1 = 800$ cm^{-1} and $h\nu = 250$ cm^{-1} in this calculation. In exploring the upper limits for $|S_\theta|$ and β, it was found that a good fit to the data may be obtained using high values for these. However, in order to keep the overall Jahn−Teller radius at the observed value, unreasonable estimates of the linear coupling constant and the energy of the Jahn−Teller mode were required; the effective ligand mass also had to be increased substantially. A model plot calculated with $S_\theta = -760$ cm^{-1}, $\beta = 350$ cm^{-1}, $A_1 = 650$ cm^{-1}, $h\nu = 300$ cm^{-1}, and $M = 40$ is shown as a dashed line on Figure 5a. It thus appears that, for the present compound, the warping parameter takes the value $\beta = 230 \pm 70$ cm^{-1}, with the axial strain being negative and related to β via the ratio $|S_\theta|/\beta \approx 2.2$.

The parameters obtained from the bond distances and electronic excitation energy have been used to calculate mean square displacements from the average distances as a function of temperature. As mentioned in section 3.1, mean square displacements increase with increasing disorder, *i.e.*, with increasing temperature. The calculated trends agree with those found experimentally (Table 3). For a more detailed comparison of the observed and calculated mean square displacements, the physical meaning of $\langle x^2\rangle - \langle x\rangle^2$, *etc.*, and ΔU (Cu−O) must be considered. The calculated quantities, $\langle x^2\rangle - \langle x\rangle^2$, *etc.*, are mean square displacements from mean distances $\langle x\rangle$, *etc.*, whereas the

(29) Hitchman, M. A.; Waite, T. D. *Inorg. Chem.* **1976**, *15*, 2150.
(30) Reynolds, R. W.; Boatner, L. A.; Abraham, M.; Chen, Y. *Phys. Rev. B: Solid State* **1974**, *10*, 3802.
(31) Steffen, G.; Reinen, D.; Stratemeier, H.; Riley, M. J.; Hitchman, M. A.; Mathies, H. E.; Recker, K.; Wallrafen, F.; Nicklas, J. R. *Inorg. Chem.* **1990**, *29*, 2123.
(32) Riley, M. J.; Hitchman, M. A.; Reinen, D.; Steffen, G. *Inorg. Chem.* **1988**, *27*, 1924.
(33) Williams, F. I. B.; Krupka, D. C.; Breen, D. P. *Phys. Rev.* **1969**, *179*, 255.
(34) Reinen, D.; Krause, S. *Inorg. Chem.* **1981**, *20*, 2750.

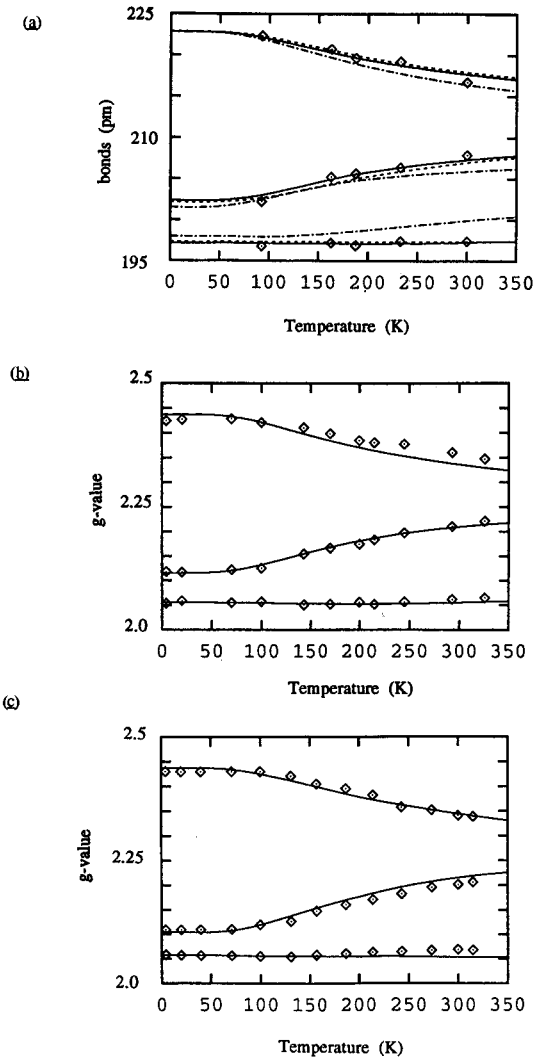

Figure 5. (a) Calculated variation of the temperature dependence of the average Cu−O bond lengths in $[Cu(thch)_2](tos)_2$ compared with the experimental values shown as diamonds. The full lines were obtained using the parameters: $A_1 = 750$ cm^{-1}, $\beta = 230$ cm^{-1}, $S_\theta = -500$ cm^{-1}, $S_\epsilon = 150$ cm^{-1}, $h\nu = 280$ cm^{-1}, $M = 25$ amu, the dashed lines using $A_1 = 650$ cm^{-1}, $\beta = 350$ cm^{-1}, $S_\theta = -760$ cm^{-1}, $S_\epsilon = 150$ cm^{-1}, $h\nu = 300$ cm^{-1}, $M = 40$ amu, and the dash−dot lines using $A_1 = 800$ cm^{-1}, $\beta = 100$ cm^{-1}, $S_\theta = -220$ cm^{-1}, $S_\epsilon = 150$ cm^{-1}, $h\nu = 250$ cm^{-1}, $M = 25$ amu. See text for the meaning of the symbols and method of calculation. (b) Comparison of the temperature dependence of the molecular *g*-values calculated using the parameters used for the full lines in a with the observed values (diamonds) for pure $[Cu(thch)_2](tos)_2$. (c) As in b but for Cu^{2+} doped $[Zn(thch)_2](tos)_2$ (∼1%).

ΔU's are obtained from the observed mean square displacements from mean positions. It thus seems that the two quantities are not directly comparable. However, the calculated quantities refer to the Jahn−Teller active ϵ_g modes (Figure 3B) in which only the ligand atoms move but not the metal atom. For these modes, the mean squared distance displacements are therefore identical to mean square positional displacements. The ΔU's, on the other hand, contain contributions from all stretching normal coordinates, *i.e.*, not only from the ϵ_g modes but also from the α_g and τ_{2u} modes. As a consequence, the ΔU's tend to be larger than $\langle x^2\rangle - \langle x\rangle^2$, *etc.*, by ∼0.002−0.003 Å^2.[11,12] If the observed values are corrected for this difference, they agree with the calculated ones to within the experimental uncertainties (Table 3).

In summary, the RHW model accounts for the Cu−O bond distances, the mean square displacements ΔU (Cu−O), and their temperature dependences as measured by X-ray diffraction.

3.3. Temperature Dependence of the *g*-Values. The way in which the EPR spectrum of $[Cu(thch)_2](tos)_2$ varies over the temperature range 4−300 K has been reported, both for the pure compound and for ∼1% Cu^{2+} doped into the corresponding Zn compound.[23] Except for the fact that the signals for the pure Cu compound are broader, very similar behavior is observed for the two systems. At low temperature, the **g**- and **A**-tensors are as expected for a Cu(II) complex with a tetragonally elongated octahedral geometry having a slight orthorhombic distortion, but as the temperature is raised, the two higher *g*-values converge so that the spectrum takes on a highly orthorhombic character. This behavior is very similar to that reported[6,9] for the Cu^{2+} doped zinc Tutton salts, and the present data were therefore interpreted using the RHW model as described[9] for these systems. The *g*-values at each temperature were estimated by calculating these for each vibronic state from the electronic part of the wave function, including spin−orbit coupling, and assuming a Boltzmann distribution over the vibronic levels. As in the previous study,[9] the treatment was not extended to include the hyperfine parameters. The behavior of these is more complicated. They depend not only on the orbital angular momentum associated with each wave function but also upon the Fermi contact interaction. Rapid electron exchange between the levels was assumed at all temperatures, as at no stage were EPR signals due to the different vibronic levels resolved. The effects of covalency were included by assigning an orbital reduction parameter *k* to each principal direction. It should be noted that the orbital reduction parameters provide an additional flexibility in the calculations not present in the fitting of the structural data, so that the latter provide a somewhat more direct probe of the potential surface.

The calculated variation of the *g*-values as a function of temperature, obtained using parameters identical to those giving optimum agreement with the X-ray data, is compared with experiment in Figure 5b for pure $[Cu(thch)_2](tos)_2$ and Figure 5c for ∼1% Cu^{2+} doped into $[Zn(thch)_2](tos)_2$. Here, the orbital reduction parameters $k_x = 0.82$, $k_y = 0.89$, and $k_z = 0.87$ were used for the pure complex, and $k_x = 0.82$, $k_y = 0.87$, and $k_z = 0.88$, for that doped in the zinc host lattice, where *x*, *y*, and *z* refer to the highest, middle, and lowest *g*-value, respectively. It is apparent that the *g*-values may be interpreted satisfactorily using the potential surface derived from the structural data. The minor deviations between the experimental and calculated values at higher temperatures may be due to a slight increase in the average *g*-value associated with the modest "red shift" of the electronic transition energies which occurs on warming. A similar effect was reported for the $CuCl_6^{4-}$ ion.[16] The orbital reduction parameters seem reasonable. The fact that $k_z \approx k_y$ is different from k_x may reflect the fact that the complex is almost tetragonally symmetric. An isotropic value $k = 0.88$ was reported for the $Cu(H_2O)_6^{2+}$ ion.[9] The very close similarity between the *g*-values and concomitant potential surface of $Cu(thch)_2^{2+}$ in the tosylate salt, and doped in the isomorphous zinc host, is consistent with the supposition that cooperative interactions in the pure compound are negligible, as assumed in both the RHW and SG models. In contrast, although the temperature dependence of the *g*-values of the $Cu(H_2O)_6^{2+}$ complex in Cu^{2+} doped zinc Tutton salts may be interpreted satisfactorily using these models,[6,9] both the *g*-values[35] and molecular geometries[20] of the pure copper(II) compounds show significant deviations at high temperature, possibly because of cooperative interactions.[20,35]

3.4. Potential Surface of the Complex and Its Vibronic Wave Functions. It is apparent that for $[Cu(thch)_2](tos)_2$ the

(35) Simmons, C. J.; Hitchman, M. A.; Stratemeier, H. Unpublished results.
(36) Hitchman, M. A. *J. Chem. Soc. A* **1970**, 4.

g-values, the deviations of the bond lengths from their mean, the mean square displacements, and the way in which all of these quantities change as a function of temperature can be explained satisfactorily using a common potential surface. A contour energy plot of the lower regions of the surface giving optimum agreement with experiment is shown on the left side of Figure 6b. The basic pattern consists of a trough at the Jahn−Teller radius, warped to give three minima with different energies. The change in energy as a function of the angle ϕ (see Figure 3A) is shown on the right side of the contour plot, plotted at the Jahn−Teller radius $\rho_0 = A_1/h\nu$. It should be noted that this gives only a schematic picture of the path of lowest energy around the "trough" in the Jahn−Teller surface, as this is not precisely circular in the presence of higher order coupling terms (Figure 6). However, the effect of the lattice strain is clearly seen—the minima in the surface are rendered inequivalent in energy and shifted from the positions corresponding to ideal 4 + 2 coordination ($\phi = 0°$, 120°, 240°).

The angular position of the lowest energy minimum ($\phi = 126°$) corresponds to a modest orthorhombic distortion imposed upon the basic tetragonally distorted octahedral geometry commonly observed for six-coordinate copper(II) complexes. Coincident with this orthorhombic distortion is a significant mixing of the electronic basis functions. It is formally impossible to extract an electronic wave function of the form shown in eq 1b from a calculated vibronic wave function as given in eq 3. However, the expectation values $\langle a^2\rangle$, $\langle b^2\rangle$, and $\langle ab\rangle$ (eq 3) may be estimated[9] and used to obtain the expectation values of the squares of the coefficients of the electronic wave function (eq 9)[36] via the relationships in eq 10. The parameters $\langle c^2\rangle$,

$$\psi_e \propto cx^2 + ey^2 + fz^2 \tag{9}$$

$$\langle c^2\rangle = 3\langle a^2\rangle - \sqrt{3}\langle ab\rangle + \langle b^2\rangle$$

$$\langle e^2\rangle = 3\langle a^2\rangle + \sqrt{3}\langle ab\rangle + \langle b^2\rangle$$

$$\langle f^2\rangle = 4\langle b^2\rangle \tag{10}$$

$\langle e^2\rangle$, and $\langle f^2\rangle$ represent the probability that the unpaired electron is found in the orbital lobes d_{x^2}, d_{y^2}, and d_{z^2}, respectively. The *z* axis is defined by the lattice strain, the negative sign of S_θ corresponding to a compression along *z*. The bond lengths, electronic wave function parameters, and *g*-values of the four lowest vibronic levels are listed in Table 4. It may be seen that for the potential surface giving optimum agreement with experiment the electronic component of the lowest vibronic level has a large lobe along *z*, a somewhat smaller one along *y*, and a very small lobe along *x*, approximately corresponding to a $d_{z^2-y^2}$ wave function. As expected, the length of each bond is correlated inversely with the magnitude of the coefficient. The wave functions of the first two excited vibronic levels differ significantly from that of the lowest level, with the bond lengths and squares of the electronic coefficients along *x* and *y* being approximately equal. For these levels the vibronic wave functions are strongly delocalized and almost intermediate between $d_{y^2-z^2}$ and $d_{x^2-y^2}$. Thus, in this respect, the conditions inherent in the SG model of the dynamic behavior of the compound do not appear to be satisfied (see following section). However, the third excited vibronic level is quite similar to the ground state, so that this simply represents an upper vibrational state of the radial component of the parent ϵ_g mode.

The energy contour plots and circular Jahn−Teller potential energy surfaces corresponding to lower and higher values of β and $|S_\theta|$, $\beta = 100$ cm^{-1}, $S_\theta = -220$ cm^{-1} and $\beta = 350$ cm^{-1}, $S_\theta = -750$ cm^{-1}, are shown in Figures 6a,c, respectively, and the corresponding bond lengths, electronic wave function

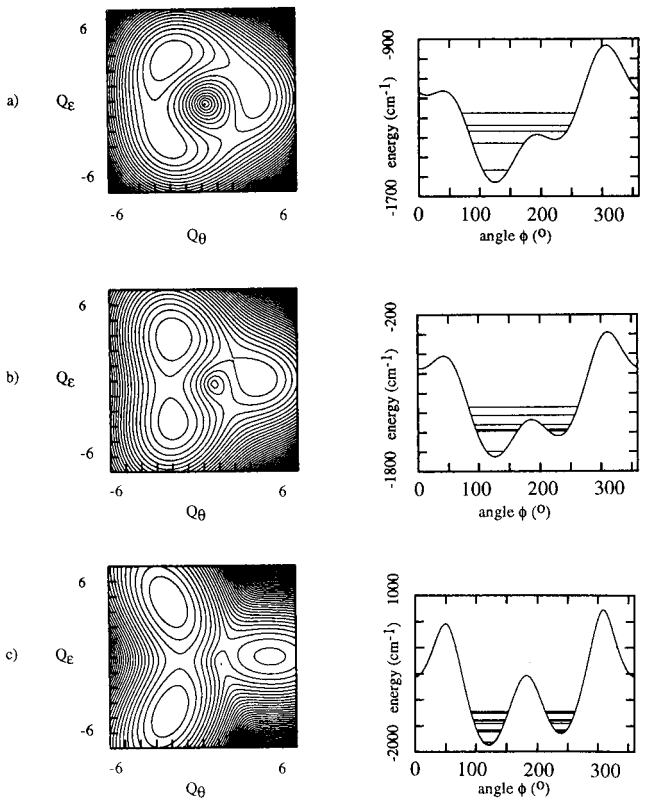

Figure 6. Left: Contour energy plots of the lower region of the potential surface (the spacing between each curve represents 100 cm^{-1}). Right: Variation of the potential energy as a function of coordination geometry at a fixed Jahn−Teller radius (see text for details). Several of the lowest vibronic energy levels are shown. The parameters defining each potential surface are (a) $A_1 = 800$ cm^{-1}, $\beta = 100$ cm^{-1}, $S_\theta = -220$ cm^{-1}, $S_\epsilon = 150$ cm^{-1}, $h\nu = 250$ cm^{-1}, $M = 25$ amu; (b) $A_1 = 750$ cm^{-1}, $\beta = 230$ cm^{-1}, $S_\theta = -500$ cm^{-1}, $S_\epsilon = 150$ cm^{-1}, $h\nu = 280$ cm^{-1}, $M = 25$ amu; and (c) $A_1 = 650$ cm^{-1}, $\beta = 350$ cm^{-1}, $S_\theta = -760$ cm^{-1}, $S_\epsilon = 150$ cm^{-1}, $h\nu = 300$ cm^{-1}, $M = 40$ amu.

parameters, and *g*-values of the four lowest vibronic levels of each surface are also given in Table 4. It is apparent that a decrease in β produces a greater delocalization of the wave functions. However, when β is increased substantially, the minima in the potential surface become more sharply defined (Figure 6c), and this causes the lower vibronic wave functions to become quite strongly localized. The relatively high value of the warping parameter β is consistent with the fact that $[Cu(thch)_2](tos)_2$ contains isolated complexes. It has been suggested that low values of this parameter are to be expected when the copper(II) is coupled to neighboring metal ions via bridging ligands,[28] and this appears to be confirmed by experiment. Values of β of less than 150 cm^{-1} have been deduced for Cu^{2+} doped into a range of continuous lattices,[30−32] while the estimates $\beta \approx 300$ and $\sim$350 cm^{-1} have been reported for the isolated complexes $Cu(H_2O)_6^{2+}$ and $CuCl_6^{4-}$, respectively.[9,16]

An independent check that the optimum strain values are reasonable (Table 4, surface 2), is provided by the metal−oxygen bond lengths observed for the compounds $[M(thch)_2](tos)_2$, M = Zn, Ni. Within the framework of the RHW model, the parameters S_θ, S_ϵ represent the strain acting on the hypothetical octahedral copper(II) complex in the absence of vibronic coupling effects. While it must be born in mind that in reality these are "effective" parameters, as they are obtained from measurements on the complex *after* distortion has occurred, similar lattice interactions are expected to be present in the corresponding Jahn−Teller inactive zinc(II) and nickel(II) compounds. Assuming that the ϵ_g vibration is of comparable energy to that in the copper(II) compound, and after taking into account the differences in average bond lengths, the optimum

Table 4. Vibrational and Electronic Components of the Four Lowest Energy Vibronic Wave Functions, Calculated for Three Possible Potential Surfaces of $[Cu(thch)_2](tos)_2$[a]

	bond lengths (Å)			electronic wavefunction			*g*-values		
energy (cm^{-1})	Cu−O2	Cu−O3	Cu−O1	$\langle c^2\rangle$	$\langle e^2\rangle$	$\langle f^2\rangle$	g_x	g_y	g_z
Surface 1: $A_1 = 800$ cm^{-1}, $\beta = 100$ cm^{-1}, $S_\theta = -220$ cm^{-1}, $h\nu = 250$ cm^{-1}, $M = 25$ amu									
227	2.169	2.072	1.982	0.85	2.00	3.15	2.314	2.203	2.068
198	2.127	2.127	1.969	1.37	1.23	3.40	2.241	2.312	2.044
138	2.206	2.043	1.974	0.33	2.37	3.30	2.389	2.156	2.053
0	2.228	2.015	1.980	0.07	2.76	3.17	2.435	2.110	2.063
Surface 2 (Optimum): $A_1 = 750$ cm^{-1}, $\beta = 230$ cm^{-1}, $S_\theta = -500$ cm^{-1}, $h\nu = 280$ cm^{-1}, $M = 25$ amu									
274	2.226	2.021	1.975	0.06	2.77	3.18	2.435	2.109	2.064
225	2.120	2.134	1.969	1.49	1.14	3.37	2.225	2.324	2.048
206	2.144	2.111	1.968	1.12	1.41	3.47	2.271	2.281	2.038
0	2.228	2.023	1.972	0.05	2.70	3.26	2.437	2.116	2.056
Surface 3: $A_1 = 650$ cm^{-1}, $\beta = 350$ cm^{-1}, $S_\theta = -760$ cm^{-1}, $h\nu = 300$ cm^{-1}, $M = 40$ amu									
365.	2.228	2.022	1.973	0.02	2.75	3.22	2.472	2.104	2.054
233	2.035	2.214	1.974	2.67	0.04	3.30	2.098	2.520	2.047
205	2.227	2.023	1.973	0.03	2.72	3.25	2.470	2.108	2.052
0	2.228	2.021	1.973	0.02	2.76	3.22	2.474	2.103	2.054

[a] See text for discussion of the parameters defining the electronic wave function and the axis system for the *g*-values. In each case the orthorhombic strain component is $S_\epsilon = 150$ cm^{-1}.

values of the lattice strain parameters for $[Cu(thch)_2](tos)_2$, $S_\theta \approx -500$ cm^{-1}, $S_\epsilon = 150$ cm^{-1}, imply[9] bond lengths (Å)

Ni−O1 = 2.030 (2.047); Ni−O2 = 2.076 (2.063);
Ni−O3 = 2.063 (2.060)

Zn−O1 = 2.042 (2.049); Zn−O2 = 2.089 (2.084);
Zn−O3 = 2.075 (2.073)

Here, the experimental values are given in parentheses, and noting that the standard deviations in these are ∼0.003 Å, the agreement for the Zn^{2+} complex is very good. The fact that the observed distortion of the Ni^{2+} complex is somewhat smaller than that calculated may be related to the fact that the ionic radius of Ni^{2+} is ∼0.05 Å smaller than those of Cu^{2+} and Zn^{2+}. The signs of the bond length changes are correct, and the marked shortening of the bond to O1 associated with the axial strain is mirrored quite well, suggesting that the estimate $S_\theta \approx -500$ cm^{-1} is reasonable. This not only confirms the energy of the highest well, but also the warping parameter β, since the ratio $|S_\theta|/\beta$ can be estimated quite accurately.

The energy differences between the lowest vibronic levels in the three wells, $\delta E_{12} = 206$ cm^{-1}, $\delta E_{13} = 810$ cm^{-1} for the optimum surface (Figure 6b), are quite similar to those estimated[9] for the $Cu(H_2O)_6^{2+}$ ion in the Cu^{2+} doped zinc(II) Tutton salts. The quantity δE_{12}, which largely depends upon the orthorhombic strain component S_ϵ, can be obtained quite accurately, since it directly influences the temperature dependence of the bond lengths and *g*-values; δE_{13}, which depends mainly upon the axial strain component S_θ, is less well-defined, as it is obtained more indirectly. A lower limit of $\delta E_{13} \approx 500$ cm^{-1} is set by the fact that the lowest *g*-value and shortest bond length do not change with temperature.

3.5. Comparison with the Silver−Getz Model. The SG model, originally developed to interpret the temperature dependence of the *g*-values of Cu^{2+} doped $K_2[Zn(H_2O)_6](SO_4)_2$,[6] has subsequently been used to interpret the EPR spectra of a number of other copper compounds,[7] as well as the temperature dependence of the bond lengths observed for a range of dynamic copper(II) complexes.[14] It is therefore of interest to apply this model to the present compound and to compare the results with those obtained using the RHW model.

The SG approach assumes that the observed variation in the structures and *g*-values is caused by a temperature dependent equilibrium between complexes which have the same geometries and **g**-tensors but differ by interchange of the directions of the largest and intermediate bonds and *g*-values. The EPR spectrum and crystal structure at low temperature yield the basic molecular *g*-values and geometry, which may then be used to derive the equilibrium constant $K = n_1/n_2$ of the number of molecules in the higher and lower energy states from the *g*-values and bond lengths at higher temperatures. It is assumed that at each temperature the EPR spectra and structures are the weighted average of those corresponding to each energy state. If the populations obey Bolzmann statistics, a plot of ln *K* against $1/T$, where *T* is the absolute temperature, should give a straight line plot with zero intercept and a slope proportional to the energy of the upper state. "Least squares" plots of the *g*-values and bond lengths for pure $[Cu(thch)_2](tos)_2$ are given in Figure 7. In the latter case, a small correction was necessary to take into account the slight thermal population of the upper state at 93 K. It is apparent that the EPR and structural data obey a similar relationship, though with a rather different slope, and that to a good approximation both follow the predictions of the SG model (the correlation coefficients are 0.996 and 0.997, respectively). For the *g*-values, there is a slight deviation from linearity for the high-temperature points, and the line of best fit, while passing close to the origin, gives a small negative intercept. Possibly, this is due to the marginal increase in the average *g*-value at high temperature. The bond length changes give a good straight line plot, and in this case within experimental error the line passes through the origin.

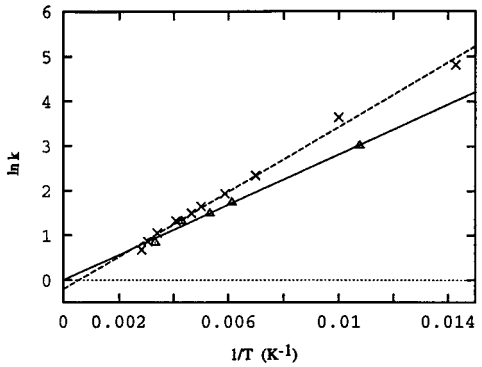

Figure 7. Plots of ln *K* against $1/T$ obtained from the *g*-values (crosses) and bond lengths (triangles) of $[Cu(thch)_2](tos)_2$, with the least squares best fit to a linear relationship shown as dashed and full lines, respectively. Here, *K* is the ratio of complexes in the upper and lower states as discussed in section 3.5, and *T* is the absolute temperature.

The SG model involves just a single upper state, the energy of this being 252 and 195 cm^{-1} as estimated from the EPR and

structural data, respectively. The "best-fit" potential surface of the RHW model, on the other hand, has the first *two* upper vibronic levels of $[Cu(thch)_2](tos)_2$ at about this energy, at 206 and 225 cm^{-1}, respectively (Table 4). Inspection of the nuclear geometries and **g**-tensor components associated with these shows that in fact neither corresponds well to the expectations of the SG approach. Instead of describing a similar geometry to that in the ground state, but with the bonds to O2 and O3 interchanged, each level corresponds to a geometry with bond lengths (and *g*-values) which are almost equivalent along these directions. The reason that the SG model produces a reasonable fit to the data with an energy separation quite similar to that of the two lower wells in the RHW approach is that the former involves a *single* upper level with two bond lengths and *g*-values reversed, while the latter involves a *pair* of delocalized upper levels, each of which differs from the lowest level by approximately *half* the amount expected in the SG approach. The thermal population of these two upper levels thus mimics that of the single upper state in the SG model.

An analogous conclusion was reached from the analysis of the temperature dependence of the *g*-values of the $Cu(H_2O)_6^{2+}$ complex in Cu^{2+} doped $Cs_2[Zn(H_2O)_6](SO_4)_2$.[9] Here the parameters defining the potential surface were found to be quite similar to those in the present complex. In particular, the lattice strain parameters $S_\theta = -650$ cm^{-1} and $S_\epsilon = 200$ cm^{-1} are close to the optimum values $S_\theta = -500$ cm^{-1} and $S_\epsilon = 150$ cm^{-1} obtained here for $[Cu(thch)_2](tos)_2$. For the Cu^{2+} doped Tutton salt, it was inferred that the delocalization of the vibronic wave functions was due to a near degeneracy of two levels and that behavior of this kind may be expected when the warping parameter β (300 cm^{-1} in the doped Tutton salt)[9] is less than or comparable to the effects of the orthorhombic component of the strain. This situation also applies for $[Cu(thch)_2](tos)_2$, and the marked influence of the warping parameter upon the geometries and *g*-values associated with the upper vibronic levels is apparent from the data listed in Table 4. For the potential surface having $\beta = 100$ cm^{-1} each of the first three excited vibronic levels involves bond lengths and *g*-values which differ significantly in magnitude from those in the ground state (surface 1). When $\beta = 350$ cm^{-1}, on the other hand, the minima in the potential surface become sharply defined and the lower vibronic wave functions are localized. Under these conditions, the SG model is obeyed rather well, and the second excited vibronic level has bond lengths and *g*-values interchanged along the *x* and *y* directions, compared with the ground level, with the first and third excited levels being virtually identical to the ground state (surface 3).

Thus, although the application of the SG model to this compound provides a good fit to the experimental data, and a calculated energy of the upper state involved in the dynamic equilibrium corresponds quite well to that of the warped potential surface deduced using the RHW model, the physical nature of the complex in its higher energy state is probably represented rather poorly by the SG model. This is in line with suggestions by Simmons,[14] who noted that when the SG model was used to interpret the temperature dependence of the geometries of the Cu^{2+} polyhedra in a range of compounds, a plot of ln *K* against $1/T$ generally gives a negative intercept, rather than a straight line passing through the origin, with the deviation becoming larger as the energy of the upper state increases. Since increased delocalization is expected as the energy of the upper state rises, it was concluded that the negative intercept may be caused by the delocalization of the wave function associated with the upper well of the Jahn−Teller potential surface. However, in the present study, where the calculations suggest significant delocalization of the wave functions in the upper well, the intercept is small for the plot of the EPR data and insignificant for that of the X-ray data (Figure 7).

4. Conclusions

For the first time, the temperature dependence of the molecular geometry and *g*-values of a copper complex have been successfully interpreted simultaneously in terms of a thermal equilibrium between the vibronic wave functions of a copper(II) complex perturbed by Jahn−Teller coupling and low-symmetry interactions with the surrounding crystal lattice. The data can also be interpreted satisfactorily using a simpler model, involving a temperature dependent equilibrium between two conformers differing solely in the orientation of the complex in the lattice. However, in the more sophisticated approach, the higher energy states participating in the thermal equilibrium involve vibronic wave functions which correspond to geometries differing significantly from that in the ground state. Thus, as far as this aspect is concerned, the simple model may be unrealistic.

Very often it is impossible to probe both the electronic and nuclear wave functions of Jahn−Teller distorted systems, and the success of the above approach suggests that results deduced from one type of measurement may be extended realistically to the overall properties of the complex. For example, the geometries of copper(II) complexes usually cannot be determined directly from the *g*-values of an EPR experiment. The present results lend confidence to the use of the RHW model to predict this aspect reasonably accurately if the average geometry is known. Similarly, chromium(II) complexes often exhibit structural properties quite similar to those of the corresponding copper(II) complexes[37] but do not give simple EPR spectra to allow characterization of the electronic wave functions. Hopefully, this may be achieved using a simple extension of the present model.

The current study involved a compound chosen so that cooperative interactions between the complexes are likely to be negligible. However, many pure copper(II) compounds exhibit dynamic behavior which differs significantly from that expected from simple Boltzmann statistics, and it has been conjectured that this is due to cooperative effects.[20,38] The success of the RHW model on the present isolated complexes means that it should be possible to extend the approach with confidence to describe the behavior of complexes coupled by cooperative interactions.

Acknowledgment. Financial support from the the Schweizerischen Nationalfonds (HBB), and the Alexander von Humboldt Foundation and Australian Research Council (MAH) is acknowledged.

Supporting Information Available: Tables giving full experimental details for all crystal structure determinations, atomic coordinates and thermal parameters for all atoms and bond lengths and angles for all complexes (33 pages). Ordering information is given on any current masthead page.

IC960343R

(37) Figgis, B. N.; Kucharski, E. S.; Reynolds, P. A. *Acta Crystallogr.* **1990**, *B46*, 577. Figgis, B. N.; Kucharski, E. S.; Forsyth, J. B. *Acta Crystallogr.* **1991**, *C47*, 419.

(38) Maaskant, W.; van der Plas, J.; Stratemeier, H.; Hitchman, M. A. Unpublished results.